

Detection of the phenomenon of turbulent thermal diffusion in numerical simulations

Nils Erland L. Haugen,^{1,*} Nathan Kleeorin,^{2,†} Igor Rogachevskii,^{2,‡} and Axel Brandenburg^{3,4,§}

¹*Sintef Energy Research, N-7034 Trondheim, Norway*

²*Department of Mechanical Engineering, Ben-Gurion University of the Negev, P.O.Box 653, Beer-Sheva 84105, Israel*

³*NORDITA, AlbaNova University Center, Roslagstullsbacken 23, SE-10691 Stockholm, Sweden*

⁴*Department of Astronomy, Stockholm University, SE 10691 Stockholm, Sweden*

(Dated: April 20, 2019, Revision: 1.49)

The phenomenon of turbulent thermal diffusion causing a non-diffusive turbulent flux of particles in the direction of the turbulent heat flux, is found using direct numerical simulations (DNS) in temperature-stratified turbulence. In simulations with and without gravity, a peak in the particle number density is found around the minimum of the mean fluid temperature for small Stokes numbers due to the phenomenon of turbulent thermal diffusion. This implies that this phenomenon causes formation of large-scale inhomogeneities in the spatial distribution of particles. For Stokes numbers larger than unity, this effect decreases with increasing Stokes number.

PACS numbers: 47.27.tb, 47.27.T-, 47.55.Hd, 47.55.Kf

Transport and mixing of particles by turbulent fluid flow is of fundamental significance in a large variety of applications (environmental sciences, physics of the atmosphere and meteorology, industrial turbulent flows and turbulent combustion, see, e.g., [1, 2]). Turbulent diffusion causes destruction of large-scale inhomogeneities in the spatial distributions of particles, while the opposite effect, turbulent thermal diffusion in temperature-stratified turbulence, can cause the formation of inhomogeneous structures in the particle density due to the appearance of a turbulent non-diffusive flux of particles in the direction of the turbulent heat flux. Turbulent thermal diffusion has been predicted theoretically in [3] and detected in different laboratory experiments in stably and unstably temperature-stratified turbulence [4–6].

The mechanism of turbulent thermal diffusion for inertial particles with material density much larger than the fluid density, is as follows [3]. The inertia causes particles inside the turbulent eddies to drift out to the boundary regions between eddies. These regions have low vorticity, high strain rate and maximum fluid pressure [7]. There is also an outflow of particles from regions with minimum fluid pressure. In homogeneous and isotropic turbulence without mean gradients of temperature, a drift from regions with increased concentration of particles by a turbulent flow is equiprobable in all directions, and the pressure (temperature) of the surrounding fluid is not correlated with the turbulent velocity field. In temperature-stratified turbulence, fluctuations of fluid temperature and velocity are correlated due to a non-zero turbulent heat flux. Fluctuations of temperature cause pressure fluctuations, which result in fluctuations of the number density of particles. Increase of the pressure of the surrounding fluid is accompanied by an accumulation of particles, and the direction of the mean flux of particles coincides with that of the turbulent heat flux. The mean flux of particles is directed toward the minimum of the mean temperature, and the particles tend to be

accumulated in this region [3].

The equation for the mean number density N of particles advected by turbulent flow has been derived using different approaches in [3, 8–11], and is given by:

$$\frac{\partial N}{\partial t} + \nabla \cdot [N (\mathbf{W}_g + \mathbf{V}^{\text{eff}}) - D_T \nabla N] = 0, \quad (1)$$

where $\mathbf{V}^{\text{eff}} = -\tau_f \overline{\mathbf{U}_p (\nabla \cdot \mathbf{U}_p)} = -\alpha D_T \nabla \bar{T} / \bar{T}$ is the effective particle velocity due to turbulent thermal diffusion, \bar{T} is the mean temperature, D_T is the turbulent diffusion coefficient, τ_f is the turbulent integral timescale, overbars mean ensemble averaging, $\mathbf{W}_g = \tau_p \mathbf{g}$ is the terminal fall velocity of particles, \mathbf{U}_p is the particle velocity, \mathbf{g} is the gravitational accelerations, τ_p is the Stokes time, and Eq. (1) is written for a zero mean velocity. The coefficient α is unity for non-inertial particles, while for inertial particles α is a function of Stokes number [3, 11]. Both the non-diffusive mean flux of particles, $N \mathbf{V}^{\text{eff}}$, and the turbulent heat flux are directed toward the mean temperature minimum. This is the reason for the formation of large-scale inhomogeneous distributions of particles.

The phenomenon of turbulent thermal diffusion is shown to be important for atmospheric flows [11] and for small-scale particle clustering in temperature-stratified turbulence [6], but it is also expected to be of large significance for different kinds of heat exchangers (e.g., industrial boilers where the Reynolds numbers and temperature gradients are large). In spite of the fact that turbulent thermal diffusion has already been found in different types of laboratory experiments [4–6], this effect has never been observed in direct numerical simulations (DNS). The main goal of this Letter is to describe the detection of the phenomenon of turbulent thermal diffusion in DNS, and to show the dependence of the turbulent thermal diffusion parameter on the Stokes number.

Equations for the fluid are solved by employing DNS in an Eulerian framework, while the equation of motion of the particles is solved in a Lagrangian framework. All numerical simulations have been performed using the Pencil

Code [12] (for details of the code, see Refs. [13, 14]). The following set of compressible hydrodynamic equations is solved for the fluid density ρ , the fluid velocity \mathbf{U} , and the specific entropy s :

$$\frac{D \ln \rho}{Dt} = -\nabla \cdot \mathbf{U}, \quad (2)$$

$$\frac{D\mathbf{U}}{Dt} = -\frac{1}{\rho} [\nabla p - \nabla \cdot (2\rho\nu\mathbf{S})] + \mathbf{f}, \quad (3)$$

$$T \frac{Ds}{Dt} = \frac{1}{\rho} \nabla \cdot K \nabla T + 2\nu\mathbf{S}^2 - c_P(T - T_{\text{ref}}), \quad (4)$$

where T is the fluid temperature, c_P is the specific heat, $D/Dt = \partial/\partial t + \mathbf{U} \cdot \nabla$, is the advective derivative, ν is the kinematic viscosity, $\rho\mathbf{f}$ is the external forcing function, p is the fluid pressure, K is the coefficient of the thermal conductivity, and $T_{\text{ref}} = T_0 + \delta T \exp(-z^2/2\sigma^2)$. The traceless rate of strain tensor is given by $S_{ij} = \frac{1}{2}(U_{i,j} + U_{j,i}) - \frac{1}{3}\delta_{ij}\nabla \cdot \mathbf{U}$. The last term in the entropy equation determines the cooling, which causes the fluid temperature minimum at $z = 0$. The size of the simulation domain is $L = 2\pi$ in all three directions and the width of the cooling function is $\sigma = 0.5$. Furthermore the strength of the cooling function, δT , is such that the relative contrast between temperature maximum and temperature minimum is ~ 1.6 . In all simulations the Prandtl number is unity.

Turbulence in the simulation box is produced by the forcing function which injects energy along a wavevector whose direction changes every timestep, but its length is approximately k_f . More details on the forcing function is found in [15]. The strength of the forcing is set such that the maximum Mach number is below 0.5, so as to be close to the incompressible limit. It has been checked that decreasing the Mach number does not have any significant effect on the results.

Particles are treated as point particles (point-particle approximation). We also consider the one-way coupling approximation, i.e., there is an effect of the fluid on the particles only, while the particles do not influence the fluid motions. This is a good approximation for small particles with low spatial number densities. The particle evolution equation reads

$$d\mathbf{U}_p/dt = \mathbf{g} - \tau_p^{-1}(\mathbf{U}_p - \mathbf{U}) \quad (5)$$

for the particle velocity and $d\mathbf{X}/dt = \mathbf{U}_p$ for the position, where $\tau_p = Sd^2/[18\nu(1 - f_c)]$ is the Stokes time, $f_c = 0.15\text{Re}_p^{0.687}$ [2], d is particle diameter and $\text{Re}_p = |\mathbf{U}_p - \mathbf{U}|d/\nu$ is the particle Reynolds number. The parameter f_c is used in order to allow for particle Reynolds numbers larger than unity. The ratio between the particle material density and the fluid mass density is $S = \rho_p/\rho$ and for all simulations $S = 1000$ outside the cooled zone. The Stokes number $\text{St} = \tau_p/\tau_k$ is based on the particle Stokes time and the Kolmogorov timescale $\tau_k = \tau_f/\sqrt{\text{Re}}$, where $\tau_f = 1/u_{\text{rms}}k_f$ is the turbulent integral timescale, $\text{Re} =$

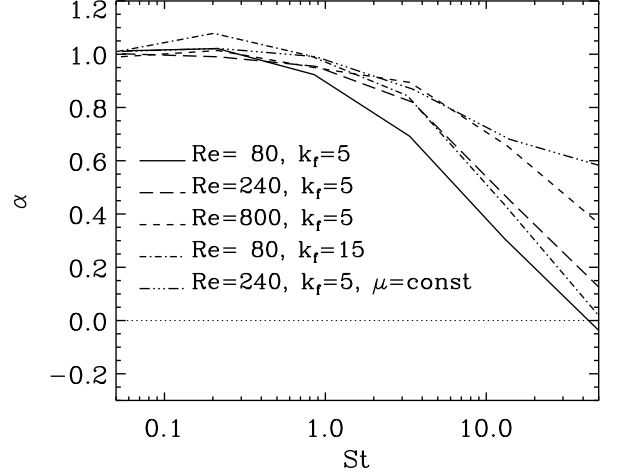


FIG. 1. The parameter α versus the Stokes number St for different Reynolds numbers and forcing wavenumbers in the absence of gravity. For the dashed-triple-dotted line the dynamic viscosity, $\mu = \rho\nu$, is kept constant while for all other lines the kinematic viscosity ν is kept constant.

$u_{\text{rms}}/\nu k_f$ is the Reynolds number and u_{rms} is the root mean square velocity. It has been checked that adding small Brownian diffusion of particles does not affect the results.

In simulations without gravity, periodic boundary conditions are used in all directions both for the fluid and for the particles. When gravity is taken into account in simulations, particles are made elastically reflecting from the vertical boundaries. Note that in all our simulations, gravity is ignored in Eq. (3) for the fluid, but it is included in Eq. (5) for particle motions. This situation has direct applications to atmospheric turbulence with lower-troposphere temperature inversions, where the density scale height due to the gravity is about 8 km, while the characteristic temperature inhomogeneity scale inside the temperature inversions is about 500–800 m, and the integral scale of turbulence is about 50–100 m.

The steady-state solution of Eq. (1) for the mean number density of particles is given by

$$\tilde{N}(z) [\tilde{T}(z)]^\alpha = \exp \left[- \int_{z_0}^z [W_g/D_T] dz' \right], \quad (6)$$

where $W_g = |\mathbf{W}_g|$, $D_T = u_{\text{rms}}/3k_f$ is the turbulent diffusion coefficient, the non-dimensional mean temperature is defined as $\tilde{T} = \bar{T}/\bar{T}_0$, while the non-dimensional mean number density of particles is $\tilde{N} = N/N_0$, where the subscripts 0 represents the values at the boundary.

In the absence of gravity, $\mathbf{W}_g = 0$ and the parameter α is given by $\alpha = -\ln \tilde{N}/\ln \tilde{T}$; see Eq. (6). In Figure 1 the Stokes number dependence of the parameter α is shown for different Reynolds numbers and different forcing scales in the absence of gravity. It can be seen that

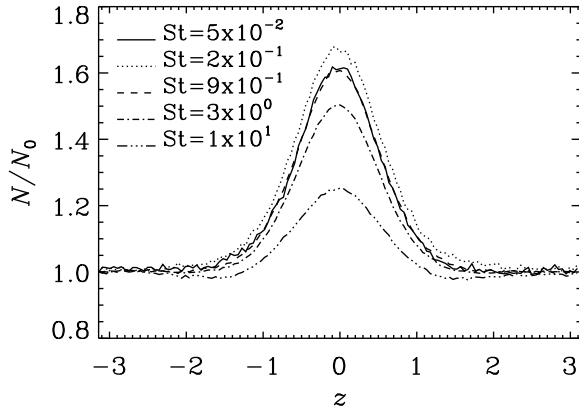


FIG. 2. Vertical profile of the mean number density for different Stokes numbers for simulations with $k_f = 5$ and $Re = 240$ and no gravity.

the parameter α reaches its maximum value for $St_* \approx 0.2$, and for Stokes numbers $St > St_*$, the value of α decreases monotonically. A critical Stokes number, St_c , separating the large and small Stokes number regimes might be defined such that α is close to unity for $St < St_c$, while for $St > St_c$ α is decreasing steeply with increasing Stokes number. Since in the simulations the rms Mach number is around 0.2, the maximum value of the parameter α is slightly larger than 1. Decreasing the Mach number causes increase α due to particle inertia, e.g., in the atmospheric turbulence the Mach number is of the order of $(0.1 - 3) \times 10^{-3}$ and α is about 10 [11]. Large particles with $\tau_p \geq \tau_f$ are affected primarily by the very largest turbulent eddies in the flow. This is because the smaller turbulent eddies have turnover times much shorter than the particle's Stokes time, and they will therefore not be able to accelerate the particles. The turbulent thermal diffusion parameter α of the large particles will therefore decrease strongly with $\tau_p \propto St$, which is seen in the large Stokes number regime of Figure 1. Furthermore, it is expected that for a given particle in the large Stokes number regime, α will be independent of Re as long as u_{rms} and k_f are kept constant. Since the Stokes number is based on the Kolmogorov time τ_k and not the turnover time of the integral scale τ_f , this implies $St_c \propto \sqrt{Re}$ which is indeed what is found in Figure 1.

When experiencing a high fluid density a particle in the large Stokes number regime will more easily be accelerated by turbulence if ν is constant than if μ is constant. This is due to the fact that for constant ν a high fluid density is associated with a smaller Stokes number, while for constant μ the Stokes number is independent of fluid density. Due to this it is expected that particles with large Stokes numbers will tend to be more depleted from the high density regions when ν is constant than when μ

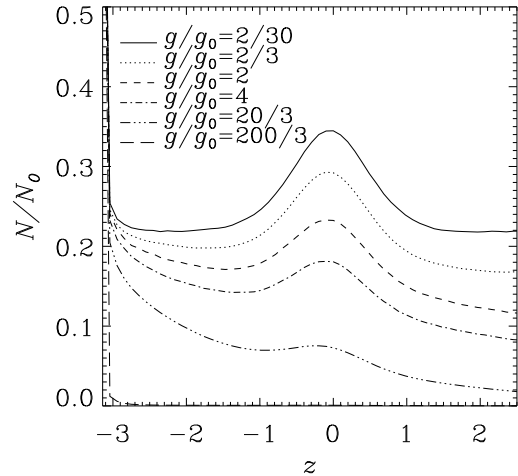


FIG. 3. Vertical profile of the mean number density for different gravitational accelerations for $St = 1$ and the forcing is at $k_f = 5.1$.

is constant. This explains why the simulation shown in Figure 1 with constant μ have a much shallower fall-off with increasing Stokes number in the large Stokes number regime than the simulations with constant ν . In Figure 2 we plot the vertical profile of the mean number density for a simulation with forcing at $k_f = 5$ and $Re = 240$ for different Stokes numbers when the kinematic viscosity is kept constant and in the absence of gravity. This corresponds to the long-dashed line in Figure 1. Particles with very large Stokes numbers are consequently found to have higher (lower) number densities in the low (high) density volume for the simulations shown in Figure 2 than for corresponding simulations with constant μ .

If the integral scale is close to the scale of the thermal cooling a particle trapped inside a turbulent eddy might travel across the whole cooled zone during one eddy turnover time. This will effectively smear out the peak of the particle number density, and consequently also decrease the parameter α . For simulations with $k_f = 5$, the integral scale is comparable to the cooling scale, and it is therefore found in Figure 1 that the peak of α is lower than for simulations with $k_f = 15$. This trend is expected to continue for yet smaller k_f .

For larger Stokes numbers, gravity plays a crucial role, and must be included in the simulations. In Figure 3, the mean particle number density is shown as a function of vertical position z for simulations with a Stokes number of unity, forcing at $k_f = 5$, and different gravitational accelerations. As the gravitational acceleration is increased, the particle number density profile is more and more tilted, as expected. In the following, gravity is nondimensionalized with $g_0 = D_T/(\tau_p L)$, so that $g/g_0 = L/L_g$, where $L_g = D_T/W_g$ is the characteristic

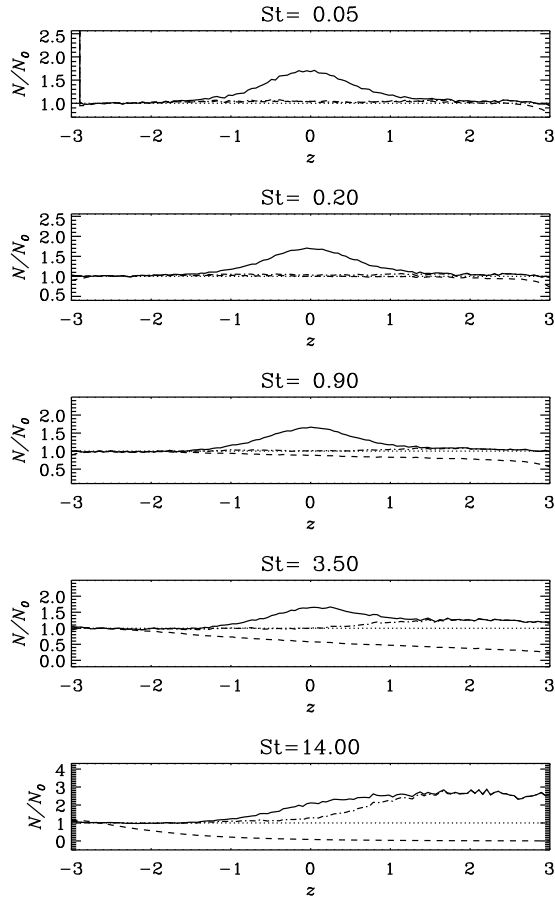


FIG. 4. Vertical profile of the mean number density for $g/g_0 = 2/3$, $k_f = 5$ and different Stokes numbers. The dotted line represent the isothermal reference case and all profiles have been normalized by this reference. The dashed line is given by the right-hand side of Eq. (6). The solid line is $N(z)$, while the dashed-dotted line is given by the left-hand side of Eq. (6), where $\alpha = 1.0, 1.0, 1.0, 0.8, 0.5$ for the five Stokes numbers starting with the smallest one. These values of α give the best fit.

scale of the mean particle number density variations due to the gravity for an isothermal case and L is the height of the box. For $g/g_0 = 200/3$ we see in Figure 3 that almost all particles have accumulated at the lower wall. In Figure 4, the vertical profile of the particle number density is shown for $g/g_0 = 2/3$ and five different Stokes numbers. The dotted line represent the isothermal case, and serves as a reference. All lines are normalized by this reference. The dashed line is given by the right-hand side of Eq. (6). The solid line is given by $\tilde{N}(z)$, while the dashed-dotted line is given by the left-hand side of Eq. (6), where the value of α is chosen in order to give the best fit to the reference isothermal case. For the three smallest Stokes

numbers in Figure 4, the parameter α is about 1, while for $St = 3.5$ and $St = 14$ a best fit of α is found around 0.8 and 0.5, respectively.

In conclusion, our numerical simulations have demonstrated the existence of the phenomenon of turbulent thermal diffusion for different Stokes numbers, fluid Reynolds numbers and different forcing scales of turbulence. Furthermore the effect of gravity has been included in simulations. It has been shown that due to the effect of turbulent thermal diffusion, particles are accumulated in the vicinity of the mean fluid temperature minimum for small Stokes numbers – in agreement with theoretical predictions [3]. When the Stokes number is larger than unity, this effect is decreasing with Stokes number.

This work was supported in part by the Norwegian Research Council project PAFrx (186933) (NELH), and by the European Research Council under the AstroDyn Research Project 227952 (AB).

* Nils.E.Haugen@sintef.no

† nat@bgu.ac.il

‡ gary@bgu.ac.il

§ brandenb@nordita.org

- [1] A. K. Blackadar, *Turbulence and Diffusion in the Atmosphere* (Springer, Berlin, 1997).
- [2] C. T. Crowe, M. Sommerfeld and Y. Tsuji, *Multiphase flows with droplets and particles* (CRC Press LLC, NY, 1998).
- [3] T. Elperin, N. Kleeorin and I. Rogachevskii, Phys. Rev. Lett. **76**, 224 (1996); Phys. Rev. E **55**, 2713 (1997).
- [4] J. Buchholz, A. Eidelman, T. Elperin, G. Grünefeld, N. Kleeorin, A. Krein, I. Rogachevskii, Experim. Fluids **36**, 879 (2004).
- [5] A. Eidelman, T. Elperin, N. Kleeorin, I. Rogachevskii and I. Sapir-Katiraie, Experim. Fluids **40**, 744 (2006).
- [6] A. Eidelman, T. Elperin, N. Kleeorin, B. Melnik and I. Rogachevskii, Phys. Rev. E **81**, 056313 (2010).
- [7] M. R. Maxey, J. Fluid Mech. **174**, 441 (1987).
- [8] T. Elperin, N. Kleeorin, I. Rogachevskii and D. Sokoloff, Phys. Rev. E **61**, 2617 (2000); ibid **64**, 026304 (2001).
- [9] R. V. R. Pandya and F. Mashayek, Phys. Rev. Lett. **88**, 044501 (2002).
- [10] M. W. Reeks, Int. J. Multiph. Flow **31**, 93 (2005).
- [11] M. Sofiev, V. Sofieva, T. Elperin, N. Kleeorin, I. Rogachevskii and S. S. Zilitinkevich, J. Geophys. Res. **114**, D18209 (2009).
- [12] The Pencil Code is a high-order finite-difference code (sixth order in space and third order in time); <http://pencil-code.googlecode.com>.
- [13] Johansen, A., Oishi, J. S., Mac Low, M. M., Klahr, H., Henning, T., & Youdin, A., Nature **448**, 1022 (2007).
- [14] N. E. L. Haugen and S. Kragset, J. Fluid Mech. **661**, 239-261 (2010).
- [15] N. E. L. Haugen and A. Brandenburg, Phys. Fluids **18**, 075106 (2006).